Theory of RF-plasma processes

Uwe Stöhr, Ph.D.

Version 1.0

June 2, 2020

Contents

1. Plasma Frequency

The plasma frequency ω_e is the eigenfrequency of the electrons. Without external forces they oscillate with this frequency around the ions. The derivation is simple: Assuming the electrons are shifted by a length x away from their position. The equation of motion is then

$$m_e \ddot{x} = -eE \tag{1}$$

where $m_e = 9.1 \cdot 10^{-31}\,\mathrm{kg}$ is the electron mass, $e = 1.602 \cdot 10^{-19}\,\mathrm{As}$ the elementary charge and E the electric field strength.

Using the electron density n_e in the Gauss law we get

$$E = \frac{e n_e}{\epsilon_0}\, x \tag{2}$$

where $\epsilon_0 = 8.854 \cdot 10^{-12}\,\mathrm{As/Vm}$ is the vacuum permittivity. Putting (2) into (1) gives

$$0 = \underbrace{\frac{e^2 n_e}{m_e \epsilon_0}}_{\text{eigenfrequency}} x + \ddot{x} \tag{3}$$

Out of this oscillation equation we can directly read the expression for the eigenfrequency:

$$\omega_e = \sqrt{\frac{e^2 n_e}{m_e \epsilon_0}} \tag{4}$$

Similarly to ω_e the eigenfrequencies for the ions can be determined:

$$\omega_i = \sqrt{\frac{e^2 n_i}{M \epsilon_0}} \tag{5}$$

where M is the mass of an ion. Due to the global quasi-neutrality $n_e \approx n_i$ for normal plasmas.

For a capacitively coupled plasma (CCP) RF-discharge at a pressure of a few pascals the typical electron density is in the range of $10^{16}\,1/\mathrm{m}^3$. This leads to $\omega_e = 5.6\,\mathrm{GHz}$. For O_2^--ions with $M = 5.312 \cdot 10^{-26}\,\mathrm{kg}$ we then have $\omega_{iO_2^-} = 23.36\,\mathrm{MHz}$.

2. Plasma Sheath

The sheath is the zone above the electrode and the chamber wall surface where the electron density n_e is much lower than the ion density n_i. This zone is also visible as the "dark zone" when looking into the chamber when a plasma is burning. The reason for the sheath is that the RF of $f = \omega/2\pi = 13.56\,\mathrm{MHz}$ is greater than the ion plasma frequency ω_i but below the electron plasma frequency ω_e. Therefore the electrons can

follow the electrical field while the ions cannot.[1] So at the time where the electrode is positively charged, electrons can stream out of the plasma to the electrode so that there is a region where $n_e \approx 0$ while $n_i \gg n_e$. The density distribution at the electrode/walls is schematically shown in Fig. 1.

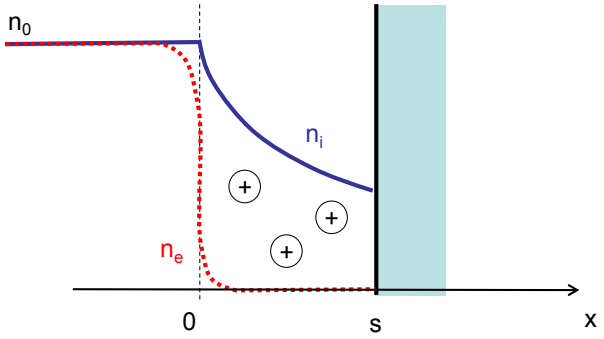

Figure 1: Scheme of the particle densities in a sheath. The wall is at $x = s$, the sheath in the range $0 \leq x \leq s$. Image from [1].

The thickness of the sheath is important to know because it determines the distance from the wall in which no substrates can be placed in for coating. It also helps to approximate the dimensions of holes and recessed areas in which strong plasma discharges will burn (hollow cathode effect). This topic is discussed in sec. 8.

2.1. Requirements for a Sheath

What is necessary to get a sheath? It is known that there is no plasma burning in small holes, so obviously there is not enough space to form a sheath. The reason could be that the ions cannot be accelerated to reach a level to build up the positive potential at the wall. That this is indeed the reason is shown in the following.

The energy conservation leads to

$$E(x) = \frac{M v_i^2(x)}{2} + e\,\Phi(x) = \frac{M v_0^2}{2} = E_0 \tag{6}$$

where M is the mass of an ion, $E(x)$ is the electric field strength in the sheath, $\Phi(x)$ the potential in the sheath, $v_i(x)$ the velocity of the ions in the sheath and v_0 the velocity of the ions in the plasma bulk streaming into the sheath.

The charge also needs to be conserved so that the current I through the area A of the sheath needs to be constant:

$$\frac{I_i}{A} = \frac{I_0}{A} = \frac{N_0 \cdot e}{tA} = n_o \cdot e \cdot v_0 \tag{7}$$

$$n_i(x) v_i(x) = n_0 v_0 \tag{8}$$

[1] **Note:** Hydrogen atoms are light enough to follow the electrical field: $\omega_{H^+} \approx 132\,\mathrm{MHz}$.

(N is the number of particles and t the time.) Putting (8) into (6) we get

$$n_i(x) = n_0 \left(1 - \frac{e\,\Phi(x)}{E_0}\right)^{-1/2} \tag{9}$$

The plasma frequency of electrons is above the applied RF so that they can follow this frequency. Therefore their density follows the Boltzmann relation:[2]

$$\begin{aligned} en_e\nabla\Phi(x) &= \nabla p(x) = \nabla n_e(x) k_B T & (10)\\ \frac{\mathrm{d}n_e(x)}{n_e(x)} &= \frac{e\,\mathrm{d}\,\Phi(x)}{k_B T_e} & (11)\\ n_e(x) &= n_0 \exp\left(\frac{e\,\Phi(x)}{k_B T_e}\right) & (12) \end{aligned}$$

with the Boltzmann constant $k_B = 1.38 \cdot 10^{-23}\,\mathrm{J/K}$.

The Gauss law is then

$$\begin{aligned} \frac{\mathrm{d}^2\Phi(x)}{\mathrm{d}x^2} &= \frac{e}{\epsilon_0}\left(n_e(x) + n_i(x)\right) & (13)\\ &= \frac{en_0}{\epsilon_0}\left(\exp\left(\frac{e\,\Phi(x)}{k_B T_e}\right) + \left(1 - \frac{e\,\Phi(x)}{E_0}\right)^{-1/2}\right) & (14) \end{aligned}$$

(ϵ_0 is the vacuum permittivity.) It cannot be solved analytically. For a derivation of an approximation at $\Phi(x \approx 0)$ see [1, sec. "Raumladungszone einer Ionenrandschicht"]. This approximation delivers the relation

$$\begin{aligned} \frac{\left(e\,\Phi(x)\right)^2}{k_B T_e} - \frac{\left(e\,\Phi(x)\right)^2}{2E_0} &> 0\\ \underbrace{\sqrt{\frac{k_B T_e}{M}}}_{v_B} &< v_0 & (15) \end{aligned}$$

v_B is named Bohm velocity and is the velocity that ions must at least have so that a sheath can be formed. This velocity is also the speed of sound of the ions.

2.2. Mean Thickness of Sheaths

We are working in a low pressure regime so that we can assume that the mean free path λ of the particles is independent of the location in the plasma chamber. For the ion

[2] See [2, sections 2.2.4 and 2.2.5] for a detailed derivation of the Boltzmann relation.

collision frequency we can now write $\nu = \frac{v_i}{\lambda}$. With the ion velocity $v_i(x) = \mu E(x)$, the ion drift mobility $\mu = \frac{e}{M\nu}$ and the field strength E we can write

$$\begin{aligned} v_i(x) &= \frac{e\lambda}{M v_i(x)} E(x) \\ &= \sqrt{\frac{e\lambda}{M} E(x)} \end{aligned} \tag{16}$$

where M is the mass of an ion and e the electron charge. The ion density can now be calculated according to (8):

$$n_i(x) = \frac{v_B}{v_i(x)} n_0 \tag{17}$$

where v_B is the BOHM velocity that is necessary to get a sheath, T_e the electron temperature, k_B the BOLTZMANN constant and $n_0 \approx n_e \approx n_i$ the density in the plasma bulk.

The simplest model of a sheath is that the electron density in the sheath is zero. Using this we can neglect the electron density n_e in the GAUSS law:

$$\epsilon_0 \frac{\mathrm{d}E}{\mathrm{d}x} = e \left(n_i(x) + \underbrace{n_e(x)}_{\approx 0} \right) = \frac{e\, n_0 \sqrt{\frac{k_B T_e}{M}}}{\sqrt{\frac{e\lambda}{M} E}} \tag{18}$$

$$\epsilon_0 \sqrt{E}\, \mathrm{d}E = e n_0 \sqrt{\frac{k_B T_e}{e\lambda}} \mathrm{d}x = j_0 \sqrt{\frac{M}{e\lambda}} \mathrm{d}x \tag{19}$$

(ϵ_0 is the vacuum permittivity and j_0 the current density.) We integrate from the border of the sheath at $x = 0$ to the chamber border at $x = s$:

$$E^3 = \frac{9}{4} s^2 n_0^2 \frac{e\, k_B T_e}{\epsilon_0^2 \lambda} \tag{20}$$

At the electrode we apply the voltage U so that we have $E(s) = \frac{U}{s}$. We can now calculate the sheath thickness s to

$$s = \left(\frac{4U^3 \epsilon_0^2 \lambda}{9 n_0^2 e k_B T_e} \right)^{1/5} \tag{21}$$

Using the relation for the mean free path assuming a MAXWELL distribution for the molecule energies

$$\lambda = \frac{k_B T}{\sqrt{2}\pi d^2 p} \tag{22}$$

(d is the diameter of the gas molecules.) (21) can be transformed to

$$s = \left(\frac{4U^3 \epsilon_0^2 T}{9\sqrt{2} n_0^2 \pi e p d^2 T_e} \right)^{1/5} \tag{23}$$

The values for λ for different precursors are listed in Appendix A. The mean voltage $\bar{U}$ at the electrode is the bias voltage so that this can be used to calculate the mean sheath thickness s.

Taking typical values: $\lambda_{O_2}(p = 2\,\mathrm{Pa}) \approx 8\,\mathrm{mm}$, $T \approx 300\,\mathrm{K}$, $T_e \approx 3 \cdot 10^4\,\mathrm{K}$, $n_0 \approx 10^{16}\,1/\mathrm{m}^3$, $p = 2\,\mathrm{Pa}$, $\bar{U} \approx 400\,\mathrm{V}$ leads with (21) to $s \approx 4.7\,\mathrm{mm}$.

(23) is the time-independent mean sheath thickness where also the dependency on the electrode area is not taken into account. An approximation of a time- and area-dependent sheath thickness is derived in the following section.

2.3. Time-dependent Thickness of Sheaths

A CCP is kept burning by shifting the charge within the chamber in the applied frequency ω_{RF}. This displacement current I_a is

$$I_a(t) = I_{\mathrm{RF}} \cos(\omega_{\mathrm{RF}} t) \tag{24}$$

I_{RF} is the current in the circuit that delivers the RF.

For the electrical field across the sheath we found the relation (20). If we this time don't integrate (19) from $x = 0..s$ but from $x = s..x$ we get

$$E(x,t)^3 = \frac{9}{4} n_0^2 \frac{e\, k_B T_e}{\epsilon_0^2 \lambda} \left(x^2 - s(t)^2 \right) \tag{25}$$

The displacement current of the sheath above a wall is

$$I_a(t) = \epsilon_0 A_w \frac{\partial E(x,t)}{\partial t} \tag{26}$$

$$= -\epsilon_0 A_w \left(\frac{9}{4} n_0^2 \frac{e\, k_B T_e}{\epsilon_0^2 \lambda} \right)^{1/3} \frac{\partial s(t)^{2/3}}{\partial t} \tag{27}$$

where A_w is the area of the wall.

With (24) we can now calculate the time-dependent $s_w(t)$:

$$s_w(t)^{2/3} = \underbrace{-\left(\frac{9}{4} n_0^2 \frac{e\, k_B T_e}{\epsilon_0^2 \lambda} \right)^{-1/3} \frac{I_{\mathrm{RF}}}{\epsilon_0 A_w \omega_{\mathrm{RF}}}}_{s_0} \sin(\omega_{\mathrm{RF}} t) + C \tag{28}$$

At one time the sheath must collapse to enable electrons to leave the plasma compensating the ion current. So at one time we have $s(t) = 0$ leading to $C = s_0$. The mean sheath thickness $\bar{s}$ is then

$$\begin{aligned}
\bar{s}_w &= \left(\frac{9}{4}\, n_0^2\, \frac{e\, k_B T_e}{\epsilon_0^2 \lambda}\right)^{-1/2} \left(\frac{I_{\mathrm{RF}}}{\epsilon_0 A_w \omega_{\mathrm{RF}}}\right)^{3/2} \underbrace{\left\langle (1-\sin(\omega_{\mathrm{RF}} t))^{3/2} \right\rangle_t}_{\approx 1.2} \\
&= \frac{2.4}{3 n_0} \sqrt{\frac{\lambda}{\epsilon_0 e\, k_B T_e}} \left(\frac{I_{\mathrm{RF}}}{A_w \omega_{\mathrm{RF}}}\right)^{3/2} \qquad (29)
\end{aligned}$$

The dime-dependent voltage across the sheath above a wall is

$$\begin{aligned}
U_w(t) &= \int_0^{s(t)} E(x,t)\, \mathrm{d}x \qquad (30) \\
&= \int_0^{s(t)} \left(\frac{9}{4}\, n_0^2\, \frac{e\, k_B T_e}{\epsilon_0^2 \lambda}\right)^{1/3} \left(x^2 - s_w(t)^2\right)^{1/3}\, \mathrm{d}x \\
&= \frac{3}{5}\, s_w(t)^{5/3} \left(\frac{9}{4}\, n_0^2\, \frac{e\, k_B T_e}{\epsilon_0^2 \lambda}\right)^{1/3} + C_U \qquad (31) \\
&= \frac{3}{5}\, \left(-s_0\, \sin(\omega_{\mathrm{RF}} t) + s_0\right)^{5/2} \left(\frac{9}{4}\, n_0^2\, \frac{e\, k_B T_e}{\epsilon_0^2 \lambda}\right)^{1/3} + C_U \\
&= \frac{3}{5}\, (1-\sin(\omega_{\mathrm{RF}} t))^{5/2} \left(\frac{I_{\mathrm{RF}}}{\epsilon_0 A_w \omega_{\mathrm{RF}}}\right)^{5/2} \left(\frac{9}{4}\, n_0^2\, \frac{e\, k_B T_e}{\epsilon_0^2 \lambda}\right)^{-1/2} + C_U \qquad (32)
\end{aligned}$$

At one time per cycle the sheath must collapse so that $U(t) = 0$. This is already the case because of the sine term so that $C_U = 0$ and we finally get

$$\begin{aligned}
U_w(t) &= \frac{2}{5 n_0 \epsilon_0^{3/2}}\, (1-\sin(\omega_{\mathrm{RF}} t))^{5/2} \left(\frac{I_{\mathrm{RF}}}{A_w \omega_{\mathrm{RF}}}\right)^{5/2} \sqrt{\frac{\lambda}{e\, k_B T_e}} \qquad (33) \\
\bar{U}_w &\approx \frac{1.92 \cdot 2}{5 n_0 \epsilon_0^{3/2}} \left(\frac{I_{\mathrm{RF}}}{A_w \omega_{\mathrm{RF}}}\right)^{5/2} \sqrt{\frac{\lambda}{e\, k_B T_e}} \qquad (34)
\end{aligned}$$

where it was used that $\left\langle (1-\sin(\omega_{\mathrm{RF}} t))^{5/2} \right\rangle_t \approx 1.92$.

But what is about the sheath at the electrode?
We know that the charge in the plasma must be conserved to fulfill the quasi-neutrality. So the current towards the wall I_a must be the opposite of the one towards the electrode

I_e. With (27) we find

$$\begin{aligned} I_a &= -I_e \\ -A_w \frac{\partial s_a(t)^{2/3}}{\partial t} &= A_e \frac{\partial s_e(t)^{2/3}}{\partial t} \\ s_e(t)^{2/3} &= -\frac{A_w}{A_e} s_a(t)^{2/3} \\ s_e(t)^{2/3} &= \frac{A_w}{A_e} \left(s_0 \sin(\omega_{\mathrm{RF}} t) - C\right) \end{aligned} \tag{35}$$

We hereby paid attention that due to the differentiation we cannot know the sign of the integration constant in (28) that we identified as $C = s_0$. The sheath thickness cannot be negative and at one time the sheath must collapse. So we get

$$\begin{aligned} s_e(t)^{2/3} &= \frac{A_w}{A_e} s_0 \left(\sin(\omega_{\mathrm{RF}} t) + 1\right) \\ s_e(t) &= \left(\frac{A_w}{A_e}\right)^{3/2} \frac{2}{3 n_0} \sqrt{\frac{\lambda}{\epsilon_0 e\, k_B T_e}} \left(\frac{I_{\mathrm{RF}}}{A_w \omega_{\mathrm{RF}}}\right)^{3/2} \left(\sin(\omega_{\mathrm{RF}} t) + 1\right)^{3/2} \qquad (36) \\ \bar{s}_e &= \left(\frac{A_w}{A_e}\right)^{3/2} \frac{2.4}{3 n_0} \sqrt{\frac{\lambda}{\epsilon_0 e\, k_B T_e}} \left(\frac{I_{\mathrm{RF}}}{A_w \omega_{\mathrm{RF}}}\right)^{3/2} = \left(\frac{A_w}{A_e}\right)^{3/2} \bar{s}_w \qquad (37) \end{aligned}$$

where it was used that $\left\langle (1 + \sin(\omega_{\mathrm{RF}} t))^{3/2} \right\rangle_t \approx 1.2$.

The voltage across the sheath at the electrode U_e can now be calculated using (31):

$$\begin{aligned} U_e(t) &= \frac{3}{5} s_e(t)^{5/3} \left(\frac{9}{4} n_0^2 \frac{e\, k_B T_e}{\epsilon_0^2 \lambda}\right)^{1/3} + C_U \\ &= \frac{3}{5} \left(\frac{A_w}{A_e}\right)^{5/2} \left(s_0 \sin(\omega_{\mathrm{RF}} t) + s_0\right)^{5/2} \left(\frac{9}{4} n_0^2 \frac{e\, k_B T_e}{\epsilon_0^2 \lambda}\right)^{1/3} + C_U \\ &= \frac{3}{5} \left(\frac{A_w}{A_e}\right)^{5/2} (1 + \sin(\omega_{\mathrm{RF}} t))^{5/2} \left(\frac{I_{\mathrm{RF}}}{\epsilon_0 A_w \omega_{\mathrm{RF}}}\right)^{5/2} \left(\frac{9}{4} n_0^2 \frac{e\, k_B T_e}{\epsilon_0^2 \lambda}\right)^{-1/2} + C_U \end{aligned} \tag{38}$$

Also in this case at one time the voltage must vanish so that $C_U = 0$ and we get

$$\begin{aligned} U_e(t) &= \left(\frac{A_w}{A_e}\right)^{5/2} \frac{2}{5 n_0 \epsilon_0^{3/2}} (1 + \sin(\omega_{\mathrm{RF}} t))^{5/2} \left(\frac{I_{\mathrm{RF}}}{A_w \omega_{\mathrm{RF}}}\right)^{5/2} \sqrt{\frac{\lambda}{e\, k_B T_e}} \\ \bar{U}_e &= \left(\frac{A_w}{A_e}\right)^{5/2} \bar{U}_w \end{aligned} \tag{39}$$

Conclusion

The wall area, the applied frequency and the input current (and thus the input power) have a strong influence on the sheath voltage, while the influence of the mean free length of path is low.

The voltage across the sheath at the electrode strongly depends on the ratio of the electrode area to the wall area. For example for the 80 l chamber device "Domino"[3] $A_w/A_e \approx 6$ so that U_e is about 88 times greater than U_w.

The expression for $\bar{U}_w$ contains with n_0 and T_e 2 variables which we usually don't measure. The electron temperature only appears because we respected that the ions in the sheath can collide with each other so that they are decelerated. As an approximation we could now neglect collisions. We then have in the sheath $n_e = 0$ and $n_i = n_0 = \text{constant}$. In this so-called "matrix sheath" model the electron temperature and the mean free path do not influence the sheath voltage and thickness.

Approximation

Using the matrix model we can write

$$\begin{aligned} \frac{\mathrm{d}\,E(x,t)}{\mathrm{d}x} &= \frac{en_0}{\epsilon_0} \\ E(x,t) &= \frac{en_0}{\epsilon_0}\,(x - s(t)) \end{aligned} \tag{40}$$

using again (26) we get

$$s_{\text{matrix}}(t) = -\underbrace{\frac{I_{\text{RF}}}{e\,n_0 A_w \omega_{\text{RF}}}}_{s_{0\,\text{matrix}}} \sin(\omega_{\text{RF}} t) + \frac{I_{\text{RF}}}{e\,n_0 A_w\,\omega_{\text{RF}}} \tag{41}$$

and

$$U_{w\,\text{matrix}}(t) = \frac{en_0}{2\epsilon_0}\, s^2_{\text{matrix}}(t) \tag{42}$$

$$= \frac{en_0}{2\epsilon_0} \left(\frac{I_{\text{RF}}}{e\,n_0 A_w\,\omega_{\text{RF}}}\,(1 - \sin(\omega_{\text{RF}} t)) \right)^2 \tag{43}$$

$$\bar{U}_{w\,\text{matrix}} = \frac{1}{2e\epsilon_0 n_0} \left(\frac{I_{\text{RF}}}{A_w\,\omega_{\text{RF}}} \right)^2 \tag{44}$$

We further on get

$$\bar{U}_{e\,\text{matrix}} = \left(\frac{A_w}{A_e} \right)^2 \bar{U}_{w\,\text{matrix}} \tag{45}$$

[3]Manufacturer: Plasma Electronic; device details: https://www.plasma-electronics.com/domino.html

3. Bias Voltage

If the electrode has the same area A_e than the area A_w of the grounded chamber walls, the voltage across both sheaths is the same. But if the electrode area is smaller, there the is less space to transport the same charge as to the chamber walls. But across the sheaths the same charge must be transported otherwise the charge conservation would be violated. This leads us to (39):

$$\bar{U}_e = \left(\frac{A_w}{A_e}\right)^{5/2} \bar{U}_w \tag{46}$$

What we measure as bias voltage is the mean voltage at the electrode

$$U_{\text{bias}} = \bar{U}_e = \bar{U}_w \left(\frac{A_w}{A_e}\right)^{5/2} \tag{47}$$

Using (34) we have

$$U_{\text{bias}} = \frac{1.92 \cdot 2}{5 n_0 \epsilon_0^{3/2}} \left(\frac{I_{\text{RF}}}{A_w \omega_{\text{RF}}}\right)^{5/2} \sqrt{\frac{\lambda}{e\, k_B T_e}} \left(\frac{A_w}{A_e}\right)^{5/2} \tag{48}$$

We know that the applied voltage (the one in the circuit) is the difference of the sheath voltages. With (33) we can therefore write

$$\begin{aligned} U_{\text{RF}}(t) &= U_e(t) - U_w(t) \\ &= \frac{2}{5 n_0 \epsilon_0^{3/2}} \left(\frac{I_{\text{RF}}}{A_w \omega_{\text{RF}}}\right)^{5/2} \sqrt{\frac{\lambda}{e\, k_B T_e}} \\ &\quad \cdot \left(\left(\frac{A_w}{A_e}\right)^{5/2} (1 + \sin(\omega_{\text{RF}} t))^{5/2} - (1 - \sin(\omega_{\text{RF}} t))^{5/2} \right) \end{aligned} \tag{49}$$

$U_{\text{RF}}(t)$, $U_w(t)$ and $U_e(t)$ are shown in Fig. 2. It can be seen that $U_e(t) - U_w(t)$ is a distorted sine that has an offset of $\left(\frac{A_w}{A_e}\right)^{5/2} - 1$ and the maximum at $\pi/2$. In our calculation we applied a cosine current. That the voltages follow a sine visualizes that the plasma sheath model treats the plasma as a pure capacity. A possible inductance due to inhomogeneities in the plasma bulk (for example if metal substrates are used) are not taken into account.

The power we have to input is

$$P(t) = I_{\text{RF}} \cos(\omega_{\text{RF}} t) \cdot U_{\text{RF}}(t) \tag{50}$$

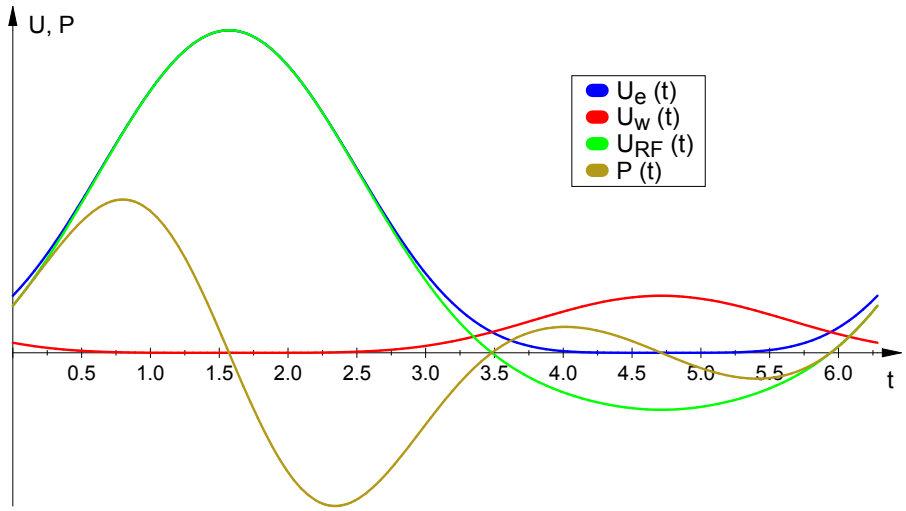

Figure 2: Temporal progression of $U_{\mathrm{RF}} = U_e - U_w$, U_e, U_e and P for $A_w/A_e = 2$.

In (49) we see that the term $(1 - \sin(\omega_{\mathrm{RF}} t))^{5/2}$ can be neglected for $\left(\frac{A_w}{A_e}\right)^{5/2} > 50$ (error is then $< 2\,\%$). Using this in (50) gives

$$P(t) = I_{\mathrm{RF}} \cos(\omega_{\mathrm{RF}} t) \frac{2}{5 n_0 \epsilon_0^{3/2}} \left(\frac{I_{\mathrm{RF}}}{A_w \omega_{\mathrm{RF}}}\right)^{5/2} \sqrt{\frac{\lambda}{e\, k_B T_e}} \left(\frac{A_w}{A_e}\right)^{5/2} (1 + \sin(\omega_{\mathrm{RF}} t))^{5/2} \quad (51)$$

The temporal progression of $P(t)$ is shown in Fig. 2. The generators measure the root mean square (RMS) of $P(t)$ as effective power. The RMS of the term $\cos(\omega_{\mathrm{RF}} t) \cdot (1 + \sin(\omega_{\mathrm{RF}} t))^{5/2}$ is ≈ 1.436. We can therefore write

$$\begin{aligned} P_{\mathrm{measured}} &= I_{\mathrm{RF}} \frac{1.436 \cdot 2}{5 n_0 \epsilon_0^{3/2}} \left(\frac{I_{\mathrm{RF}}}{A_w \omega_{\mathrm{RF}}}\right)^{5/2} \sqrt{\frac{\lambda}{e\, k_B T_e}} \left(\frac{A_w}{A_e}\right)^{5/2} \\ &= I_{\mathrm{RF}}^{7/2} \frac{1.436 \cdot 2}{5 n_0 \epsilon_0^{3/2}} \left(\frac{1}{A_e \omega_{\mathrm{RF}}}\right)^{5/2} \sqrt{\frac{\lambda}{e\, k_B T_e}} \quad (52) \\ I_{\mathrm{RF}} &= \left(\frac{1.436 \cdot 2}{5 P_{\mathrm{measured}} n_0 \epsilon_0^{3/2}} \left(\frac{1}{A_e \omega_{\mathrm{RF}}}\right)^{5/2} \sqrt{\frac{\lambda}{e\, k_B T_e}}\right)^{-2/7} \\ &= \left(\frac{5 P_{\mathrm{measured}} n_0 \epsilon_0^{3/2}}{1.436 \cdot 2}\right)^{2/7} \left(\frac{e\, k_B T_e}{\lambda}\right)^{1/7} (A_e \omega_{\mathrm{RF}})^{5/7} \quad (53) \end{aligned}$$

This could now be put into (48):

$$
\begin{aligned}
U_{\text{bias}} &= \frac{1.92 \cdot 2}{5 n_0 \epsilon_0^{3/2}} \left(\frac{\left(\frac{5 P_{\text{measured}} n_0 \epsilon_0^{3/2}}{1.436 \cdot 2} \right)^{2/7} \left(\frac{e\, k_B T_e}{\lambda} \right)^{1/7} (A_e \omega_{\text{RF}})^{5/7}}{A_w \omega_{\text{RF}}} \right)^{5/2} \sqrt{\frac{\lambda}{e\, k_B T_e}} \left(\frac{A_w}{A_e} \right)^{5/2} \\
&= \frac{0.831}{n_0 \epsilon_0^{3/2} \omega_{\text{RF}}^{5/2}} \left(\left(P_{\text{measured}} n_0 \epsilon_0^{3/2} \right)^{2/7} \left(\frac{e\, k_B T_e}{\lambda} \right)^{1/7} (A_e \omega_{\text{RF}})^{5/7} \right)^{5/2} \sqrt{\frac{\lambda}{e\, k_B T_e}} \left(\frac{1}{A_e} \right)^{5/2} \\
&= \frac{0.831}{n_0^{2/7} \epsilon_0^{3/7}} \left(\frac{P_{\text{measured}}}{\omega_{\text{RF}} A_e} \right)^{5/7} \left(\frac{\lambda}{e\, k_B T_e} \right)^{1/7} \qquad (54)
\end{aligned}
$$

and (37) but this doesn't help us as long as we don't know the electron temperature. We therefore go back to the matrix model approximation.

3.1. Approximation

We already found (43):

$$
U_{w\,\text{matrix}}(t) = \frac{e n_0}{2\epsilon_0} \left(\frac{I_{\text{RF}}}{e\, n_0 A_w \omega_{\text{RF}}} \left(1 - \sin(\omega_{\text{RF}} t)\right) \right)^2 \qquad (55)
$$

and with (45) we get

$$
U_{\text{RF}}(t) = \frac{e n_0}{2\epsilon_0} \left(\frac{I_{\text{RF}}}{e\, n_0 A_w \omega_{\text{RF}}} \right)^2 \left(\left(\frac{A_w}{A_e} \right)^2 (1 + \sin(\omega_{\text{RF}} t))^2 - (1 - \sin(\omega_{\text{RF}} t))^2 \right) \qquad (56)
$$

To calculate the power we assume that $\left(\frac{A_w}{A_e} \right)^2 \gg 1$ so that we have to find only the RMS of the term $\cos(\omega_{\text{RF}} t) \cdot (1 + \sin(\omega_{\text{RF}} t))^2$. This is ≈ 1.146 so that we can now write

$$
\begin{aligned}
P_{\text{measured}} &= I_{\text{RF}} \frac{1.146 \cdot e n_0}{2\epsilon_0} \left(\frac{I_{\text{RF}}}{e\, n_0 A_w \omega_{\text{RF}}} \right)^2 \left(\frac{A_w}{A_e} \right)^2 \\
&= I_{\text{RF}}^3 \frac{1.146}{2\epsilon_0 e n_0} \left(\frac{1}{A_e \omega_{\text{RF}}} \right)^2 \qquad (57) \\
I_{\text{RF}} &= (A_e\, \omega_{\text{RF}})^{2/3} \left(\frac{2\epsilon_0 e n_0 P_{\text{measured}}}{1.146} \right)^{1/3} \qquad (58)
\end{aligned}
$$

Putting this relation for I_{RF} into (44) gives

$$
\begin{aligned}
U_{\mathrm{bias}} &= \frac{1}{2e\epsilon_0 n_0}\left(\frac{I_{\mathrm{RF}}}{A_w\,\omega_{\mathrm{RF}}}\right)^2\left(\frac{A_w}{A_e}\right)^2 && (59)\\
&= \frac{1}{2e\epsilon_0 n_0}\left(\frac{\left(A_e\,\omega_{\mathrm{RF}}\right)^{2/3}\left(\frac{2\epsilon_0 e n_0 P_{\mathrm{measured}}}{1.146}\right)^{1/3}}{A_e\,\omega_{\mathrm{RF}}}\right)^2\left(\frac{A_w}{A_e}\right)^2\\
&= \left(\frac{1}{2e\epsilon_0 n_0}\right)^{1/3}\left(\frac{P_{\mathrm{measured}}}{1.146\cdot A_e\,\omega_{\mathrm{RF}}}\right)^{2/3}\left(\frac{A_w}{A_e}\right)^2 && (60)
\end{aligned}
$$

and this can be transformed to deliver the plasma density:

$$
\begin{aligned}
n_0^{1/3} &= \frac{1}{U_{\mathrm{bias}}}\left(\frac{1}{2e\epsilon_0}\right)^{1/3}\left(\frac{P_{\mathrm{measured}}}{1.146\cdot A_e\,\omega_{\mathrm{RF}}}\right)^{2/3}\left(\frac{A_w}{A_e}\right)^2\\
n_0 &= \frac{1}{2e\epsilon_0 U_{\mathrm{bias}}^3}\left(\frac{P_{\mathrm{measured}}}{1.146\cdot A_e\,\omega_{\mathrm{RF}}}\right)^2\left(\frac{A_w}{A_e}\right)^6 && (61)
\end{aligned}
$$

With this approximated plasma density we can also approximate the ionization ratio Γ_i:

$$\Gamma_i = \frac{N}{Vn_0} = \frac{p}{k_B T\, n_0} \tag{62}$$

where N is the number of particles in the plasma chamber, p is the pressure, V the volume of the chamber and T the global temperature in the chamber.

Although (61) is an approximation, we can put it into the precise relation (34) to get a feeling how the electron temperature behaves:

$$
\begin{aligned}
U_{\mathrm{bias}} &= \frac{1.92\cdot 2}{5n_0\epsilon_0^{3/2}}\left(\frac{I_{\mathrm{RF}}}{A_w\omega_{\mathrm{RF}}}\right)^{5/2}\left(\frac{ek_BT_e}{\lambda}\right)^{-1/2}\left(\frac{A_w}{A_e}\right)^{5/2}\\
\frac{ek_BT_e}{\lambda} &= \left(\frac{1.92\cdot 2}{5n_0\epsilon_0^{3/2}U_{\mathrm{bias}}}\left(\frac{I_{\mathrm{RF}}}{A_w\omega_{\mathrm{RF}}}\right)^{5/2}\left(\frac{A_w}{A_e}\right)^{5/2}\right)^2\\
T_e &= \left(\frac{1.92\cdot 2}{5}\right)^2\left(\frac{I_{\mathrm{RF}}}{A_e\,\omega_{\mathrm{RF}}}\right)^5\frac{\lambda}{n_0^2\,\epsilon_0^3\,U_{\mathrm{bias}}^2\,ek_B} && (63)\\
&= \left(\frac{1.92\cdot 2}{5}\right)^2\left(\frac{\left(\frac{5P_{\mathrm{measured}}n_0\epsilon_0^{3/2}}{1.436\cdot 2}\right)^{2/7}\left(\frac{e\,k_BT_e}{\lambda}\right)^{1/7}\left(A_e\omega_{\mathrm{RF}}\right)^{5/7}}{A_e\,\omega_{\mathrm{RF}}}\right)^5\frac{\lambda}{n_0^2\,\epsilon_0^3\,U_{\mathrm{bias}}^2\,ek_B}\\
&= \left(\left(\frac{1.92\cdot 2}{5}\right)^2\left(\frac{5P_{\mathrm{measured}}n_0\epsilon_0^{3/2}}{1.436\cdot 2}\right)^{10/7}\left(\frac{e\,k_B}{\lambda}\right)^{5/7}\frac{1}{\left(A_e\omega_{\mathrm{RF}}\right)^{10/7}}\frac{\lambda}{n_0^2\,\epsilon_0^3\,U_{\mathrm{bias}}^2\,ek_B}\right)^{7/2}\\
&= \left(\frac{1.92\cdot 2}{5}\right)^7\left(\frac{5P_{\mathrm{measured}}}{1.436\cdot 2}\right)^5\frac{\lambda}{n_0^2ek_B\,\left(A_e\omega_{\mathrm{RF}}\right)^5\,\epsilon_0^3\,U_{\mathrm{bias}}^7} && (64)
\end{aligned}
$$

3.2. Conclusions

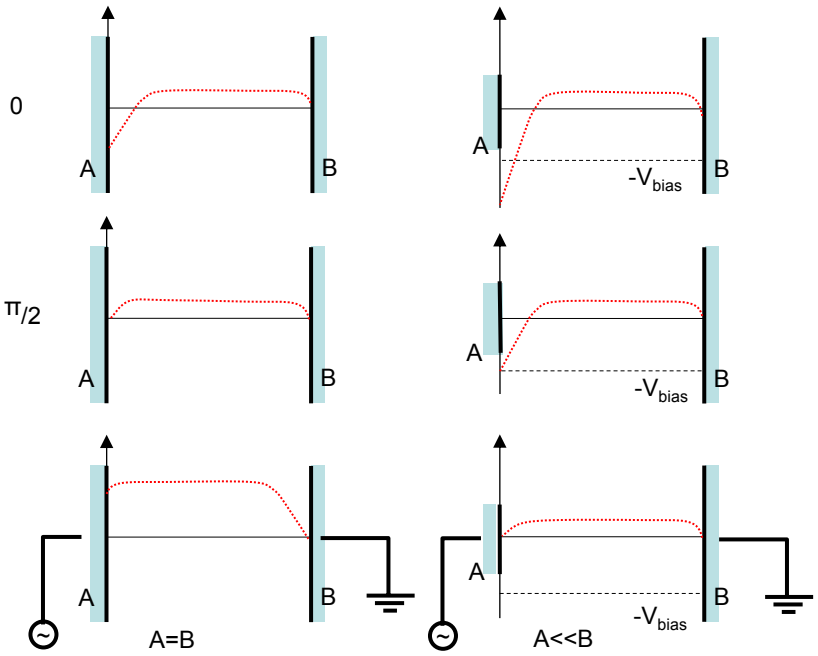

Figure 3: Spatial progression of the voltage in a plasma between symmetric and asymmetric electrode areas. Image from [1].

Fig. 3 shows the spatial progression of the voltage inside a plasma schematically. Due to the smaller electrode area the voltage across the sheath above the electrode is much higher. This is the effect we use to accelerate ions towards substrates to coat them. (48) shows that a smaller A_e leads to less necessary input current (and thus input power) to get the same bias voltage.

Interesting is the inverse cubic dependence of the bias voltage in (61). So a low plasma density results in a high bias. This is an important result because this is the reason why a dense plasma is burning into holes of substrates at the electrode for low ionized plasmas. These are typically plasmas of mainly larger precursor molecules. This topic is discussed in detail in sec. 8.

The plasma density n_0 for the 80 l chamber device "Domino"[4] is shown in Fig. 4, the plasma density for a 720 l chamber device "Porta 900"[5] in Fig. 5. One can see that if one measures for a low power a relatively high bias, the plasma density is low meaning the ionization rate is also low. By modifying the "Porta 900" so that the device chamber is divided by 3 equally sized inner chambers with each a smaller electrode, the plasma

[4]Manufacturer: Plasma Electronic; device details: https://www.plasma-electronics.com/domino.html
[5]Manufacturer: Plasma Electronic; cubic chamber with an edge length of 0.9 m;
device details: https://www.plasma-electronics.com/porta.html

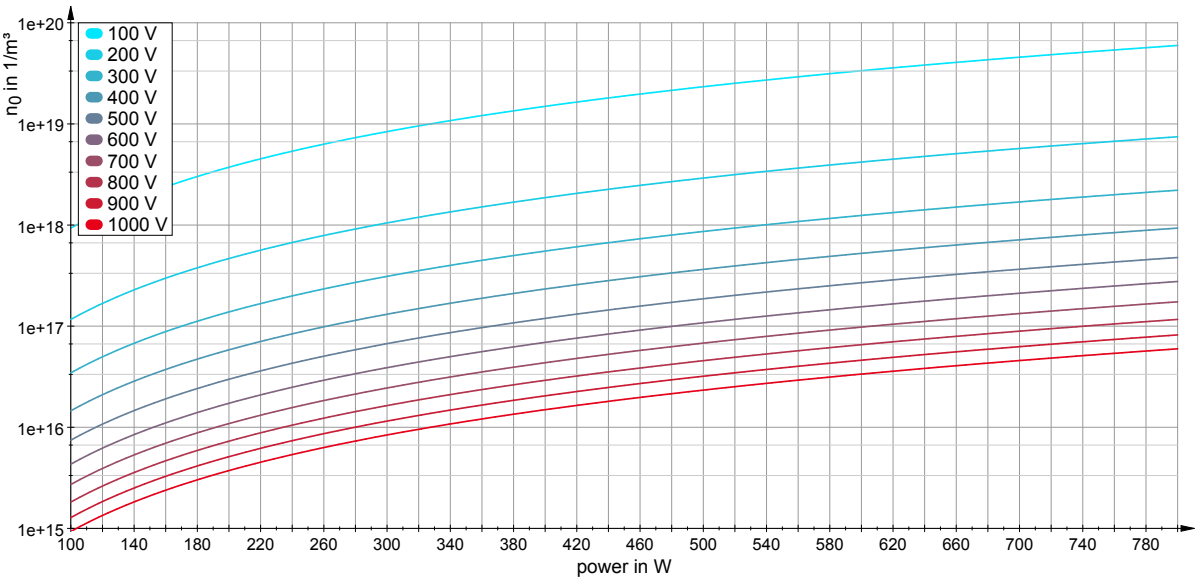

Figure 4: Plasma density for the plasma device "Domino" with a chamber volume of 80 l ($A_e \approx 0.138\,\mathrm{m}^2$, $A_w \approx 0.832\,\mathrm{m}^2$) in dependence of the applied plasma power and the measured U_{bias}.

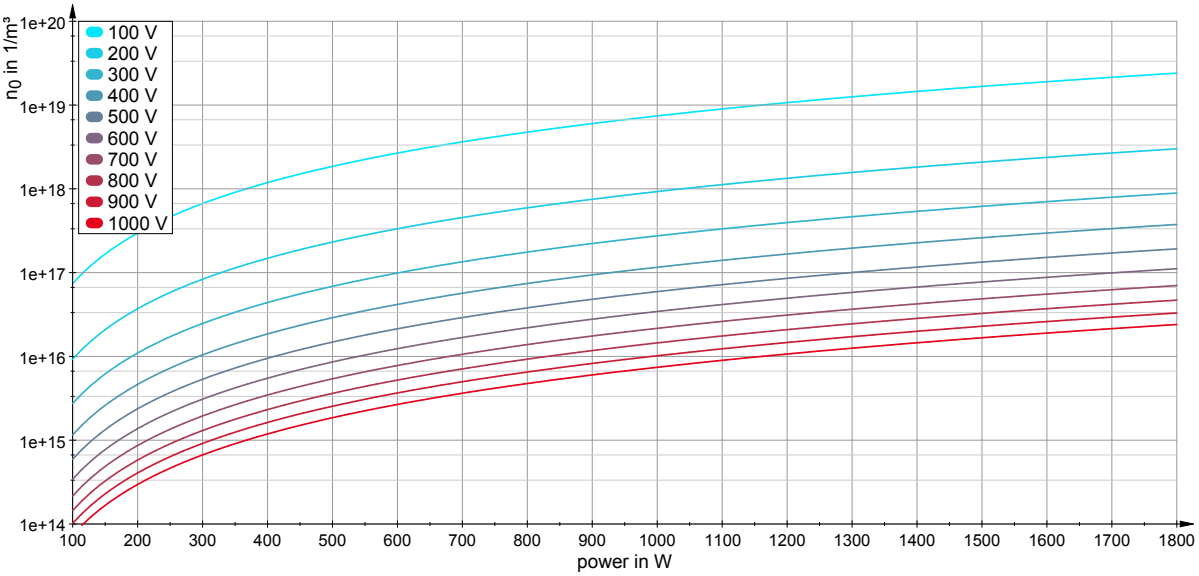

Figure 5: Plasma density for the plasma device "Porta 900" with one large electrode ($A_e = 0.64\,\mathrm{m}^2$, $A_w = 0.9^2 \cdot 6 - 0.64 = 4.22\,\mathrm{m}^2$) in dependence of the applied plasma power and the measured U_{bias}. For the setup with 3 chambers ($A_e = 0.07\,\mathrm{m}^2$, $A_w = 2.594\,\mathrm{m}^2$) the values in this plot must be multiplied with the factor 198.16.

density is increased by about a factor 200. So the then different ratio A_e/A_w change the plasma parameters drastically.

Taking the case that in the "Domino" we measured a bias of 500 V for pure Ar at $p = 2\,\mathrm{Pa}$ with a power of 190 W. With Fig. 4 we get $n_0 \approx 1.5 \cdot 10^{14}\,1/\mathrm{m}^3$ and therefore with (63) $T_e \approx 7.6 \cdot 10^5\,\mathrm{K}$. But this about 100 times higher than values found in literature and with (75) we would get a plasma potential of about 327 V. This shows that the electron temperature cannot be estimated using the matrix model in its derivation. This result could have been expected because the matrix model does not take care of T_e. In fact one cannot estimate T_e by measuring only the plasma power and the bias voltage.

3.3. Applications

3.3.1. ICP + CCP

Looking at (54):

$$U_{\mathrm{bias}} = \frac{0.831}{n_0^{2/7}\epsilon_0^{3/7}} \left(\frac{P_{\mathrm{measured}}}{\omega_{\mathrm{RF}} A_e}\right)^{5/7} \left(\frac{\lambda}{e\,k_B T_e}\right)^{1/7} \tag{65}$$

we see that $U_{\mathrm{bias}} \sim n_0^{-2/7}$, $U_{\mathrm{bias}} \sim P_{\mathrm{measured}}^{5/7}$ and $U_{\mathrm{bias}} \sim T_e^{-1/7}$. For a setup where the ions are generated in an inductively coupled plasma (ICP), the ion energy is a constant while the ion density increases with increasing input power for the ICP. To get a defined and adjustable ion impact energy on the substrate one can apply an RF-voltage to the substrate. We then have a capacitively coupled plasma (CCP) above the substrate but n_0 is almost independent of the CCP parameters.

For a glass etching application this setup was chosen. For the ICP and the CCP the same frequency was used. As both plasmas did not interfere in this setup although the same frequency was used, they can be treated as being independent from each other. Then for a constant ICP power and thus a constant n_0 the bias voltage should have the dependency $U_{\mathrm{bias}} \sim P_{\mathrm{measured}}^{5/7}$ for the case that the CCP does not change the electron temperature T_e. The measurements to prove this theory was performed using an ICP source model "Copra DN 160"[6]. The result is plotted in Fig. 6. Fitting the curves in this plot with the function $U_{\mathrm{bias}} = K \cdot P_{\mathrm{measured}}^{X}$ gives the results listed in Table 1. The expected exponent $5/7 \approx 0.71$ is the one for 300 W. For larger ICP powers the exponent increases which implies that T_e is then smaller.

Table 1: Fit parameters for the measurement curves from Fig. 6.

ICP power in W	Parameter X	Parameter K	χ^2_{red} of the fit
300	0.71 ± 0.01	73.71 ± 9.09	1.12
400	0.79 ± 0.01	22.82 ± 2.06	1.58
500	0.82 ± 0.01	14.82 ± 1.16	1.31

[6] Manufacturer: CCR technology;
device details: https://www.ccrtechnology.de/copra-products/copra-round-sources/

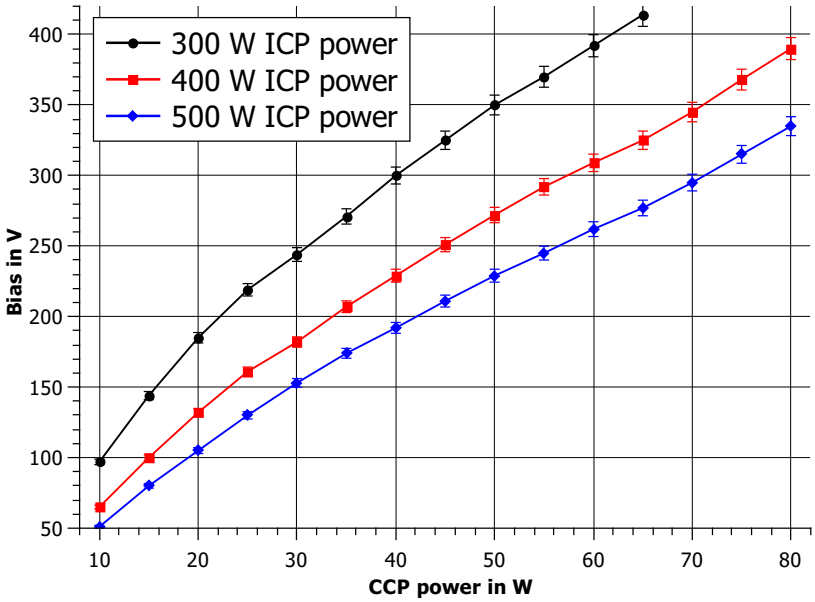

Figure 6: Dependency of the bias voltage on the CCP power for different ICP powers.

The ion current density in the used ICP source for a fixed pressure of 0.1 Pa is for an input power of 300 W about 0.1 mA/cm² and for 500 W about 0.21 mA/cm². Although we measured at a pressure of about 0.4 Pa we assume that also n_0 is increased by a factor 1.75 if going from 300 to 500 W ICP power. For low CCP powers we can neglect the influence of the CCP on n_0 and expect that the bias voltage for 500 W is $1.75^{2/7} \approx 0.44$ lower than for 300 W. Looking at Fig. 6 we get a factor 0.53 – 0.67 lower bias voltage, depending on the CCP power, see Table 2. Even for the lowest measurable CCP power of 10 W we see again that an increasing ICP power decreases T_e as the factor is much greater than expected. For higher CCP powers we have also a lower T_e. This is an interesting result because a higher CCP power always leads to a higher n_0 and this decreases the bias.

Table 2: Factors of the decreasing bias voltages when going from 300 to 500 W ICP power; in dependence of the CCP power.

CCP power in W	10	15	20	30	40	50	60
Factor	0.53	0.55	0.56	0.62	0.64	0.65	0.67

3.3.2. CCP

In contrary to the combination of ICP + CCP, for a pure CCP the Bias voltage behave differently. According to (54):

$$U_{\text{bias}} = \frac{0.831}{n_0^{2/7}\epsilon_0^{3/7}} \left(\frac{P_{\text{measured}}}{\omega_{\text{RF}} A_e}\right)^{5/7} \left(\frac{\lambda}{e\, k_B T_e}\right)^{1/7} \tag{66}$$

one gets the relations $U_{\text{bias}} \sim n_0^{-2/7}$ and $U_{\text{bias}} \sim P_{\text{measured}}^{5/7}$. In a CCP an increased P will also always result in an increased n_0 and a changed T_e. For practical applications it is helpful to know how the Bias is changed by changing the input power and the pressure p.

For the measurement the device "Labor 1" (80 liter vacuum chamber) was used. Pure argon was used as process gas because it is a single-atom gas (to keep the pressure constant because no molecule fragmentation can occur). The Bias voltage was measured at constant pressures while the input power was changed. The resulting datasets were fit using these equations

$$U_{\text{bias}} = K \cdot (P_{\text{measured}} - x_0)^{B_{\text{powerr}}} + y_0 \tag{67}$$

$$U_{\text{bias}} = K \cdot (p - x_0)^{B_{\text{pressure}}} + y_0 \tag{68}$$

Fig. 7 shows as example how the results looked. It can be seen that the fit at constant pressure well describes the change of the Bias whereas the fit at constant pressure shows that the fit model is not optimal ($\chi_{\text{red}} > 1$). In Fig. 8 the fit parameters B_{power} and B_{pressure} are plotted for the different pressures and powers, receptively. One can see that the fit parameters are relatively constant for the different pressures and powers. As final conclusion one gets for a CCP with argon:

$$U_{\text{bias}} \sim P_{\text{measured}}^{0.5360 \pm 0.0152} \tag{69}$$

$$U_{\text{bias}} \sim p^{-0.1831 \pm 0.0016} \tag{70}$$

This shows that the plasma density n_0 is indeed increased if the pressure is increased. The electron temperature T_e is increased too so that the exponent in (70) is greater than $-2/7$. If the CCP-power is increased n_0 and T_e are increased too so that the exponent in (69) is smaller than $5/7$.

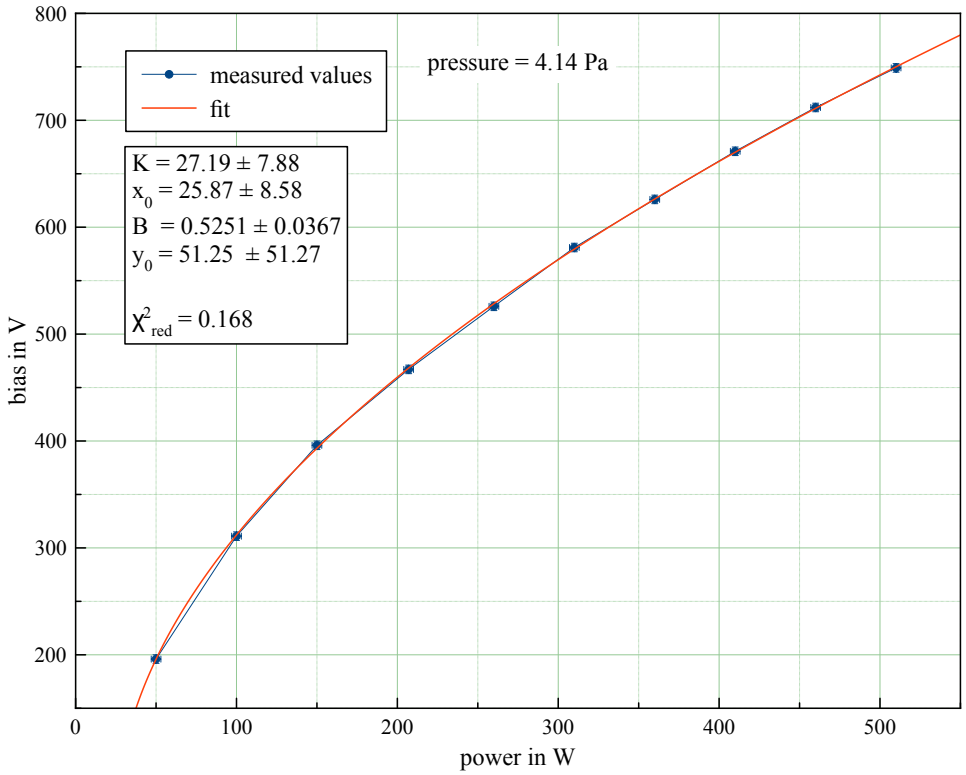

(a) Dependency of the bias voltage on the input power for a fixed pressure of 4.14 Pa.

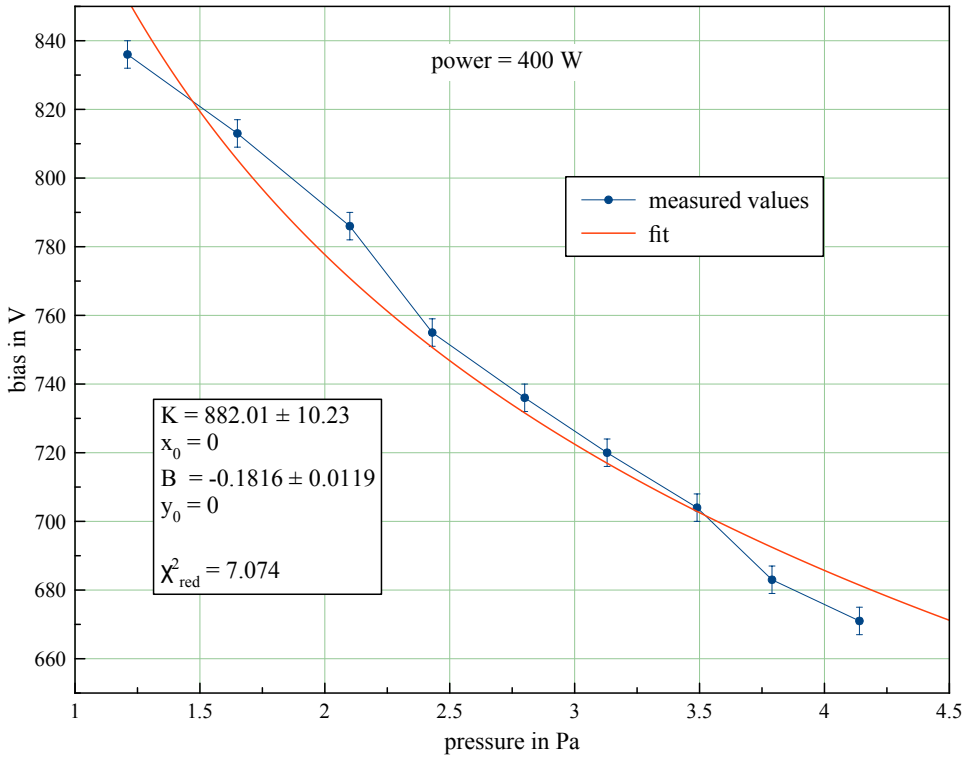

(b) Dependency of the bias voltage on the pressure for a fixed input power of 400 W.

Figure 7: Dependency of the bias voltage on the pressure and the input power for 2 different cases.

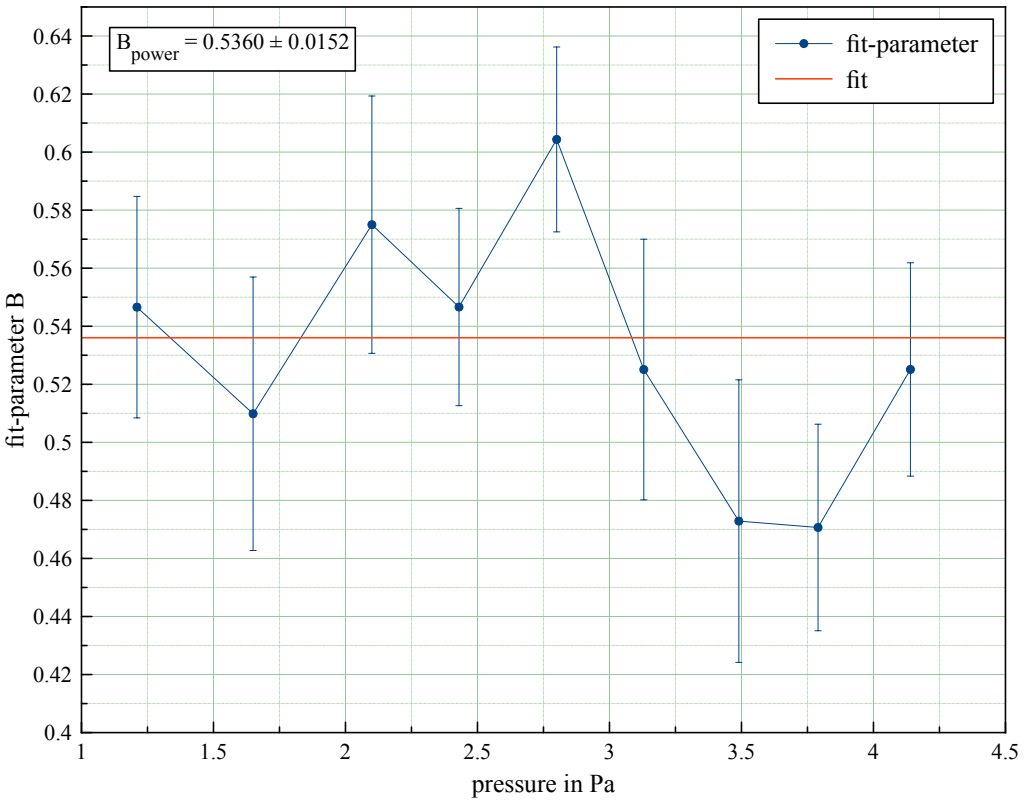

(a) Fit of the fit-parameters B_{power} at different pressures.

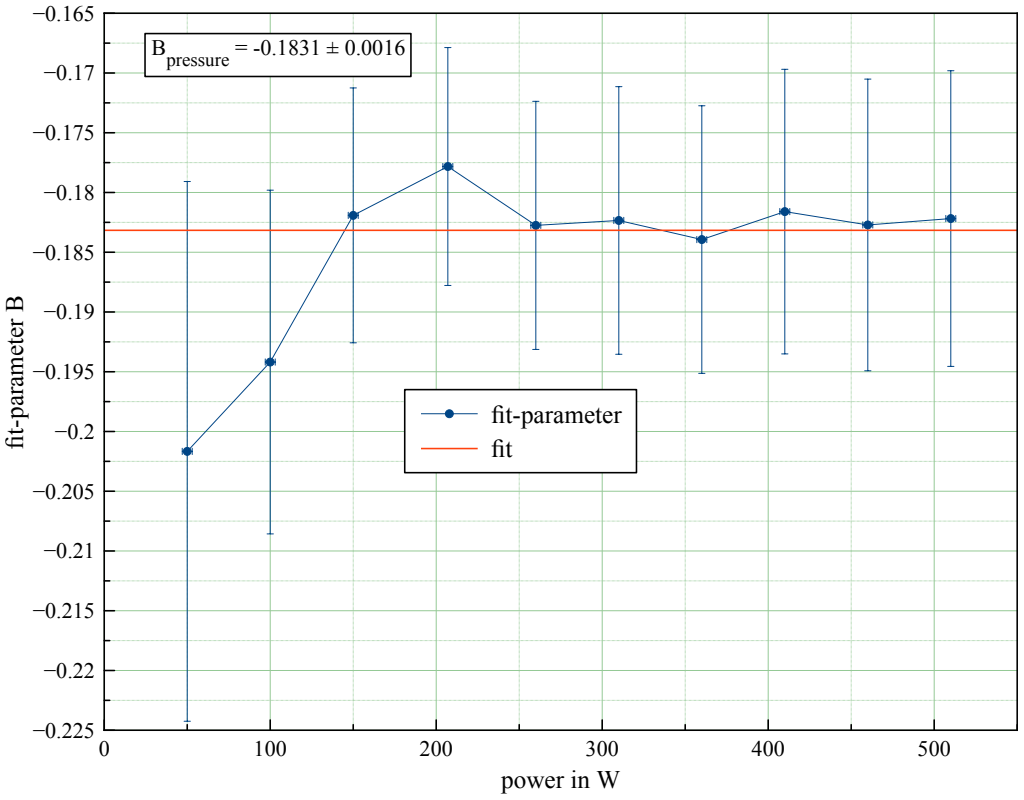

(b) Fit of the fit-parameters B_{pressure} at different input powers.

Figure 8: Linear fit of the different fit-parameters B_{power} and B_{pressure}.

4. Floating Potential

When treating polymer substrates they are often placed into the chamber without an electrical connection to the chamber walls or the electrode. At the substrate there is therefore no sheath. The question is now how large the potential between the plasma and the substrate will be.

As there is no electric connection, the substrate is on a so-called floating potential and the ion current I_i must be equal the electron current I_e onto the substrate surface. So we can write

$$\begin{aligned} I_e &= I_i \\ A\, n_0 v_{e,\,\mathrm{therm}} &= A\, n_0 v_B \end{aligned} \tag{71}$$

where we used that the ions within the plasma must have the BOHM velocity.

Within the plasma we can assume that the electrical field is independent of the position. Therefore the velocity of the electrons is their thermal one $v_{e,\,\mathrm{therm}}$.

The mean $v_{e,\,\mathrm{therm}}$ can be calculated using the Maxwell-Boltzmann distribution $f(v)$:

$$\begin{aligned} \langle v_{e,\,\mathrm{therm}} \rangle &= \int v f(v)\,\mathrm{d}v \\ &= \int v_e \sqrt{\frac{m_e}{2\pi k_B T_e}} \exp\left(\frac{-m_e v_e^2}{2 k_B T_e}\right) \mathrm{d}v_e \\ &= -\sqrt{\frac{k_B T_e}{2\pi m_e}} \exp\left(\frac{-e\,\Phi}{k_B T_e}\right) \end{aligned} \tag{72}$$

Where the relation $\dfrac{m_e v_e^2}{2} = e\,\Phi$ was used.

(71) becomes now

$$\begin{aligned} \sqrt{\frac{k_B T_e}{M}} &= -\sqrt{\frac{k_B T_e}{2\pi m_e}} \exp\left(\frac{-e\,\Phi_{\mathrm{float}}}{k_B T_e}\right) \\ \Phi_{\mathrm{float}} &= \frac{k_B T_e}{e} \ln\left(\sqrt{\frac{2\pi m_e}{M}}\right) \end{aligned} \tag{73}$$

In our devices the electrode is set to a certain voltage to apply power to the plasma. Therefore we get a bias which is negative. Electrons are therefore reflected and cannot reach the electrode surface (except of one point in time). We therefore have instead of (71)

$$A_w\, n_0 v_{e,\,\mathrm{therm}} = n_0 v_B\,(A_w + A_e) \tag{74}$$

which leads to

$$\begin{aligned}\sqrt{\frac{k_B T_e}{M}}\,(A_w + A_e) &= -\sqrt{\frac{k_B T_e}{2\pi m_e}}\exp\left(\frac{-e\,\Phi_{\text{float}}}{k_B T_e}\right) A_w \\ \Phi_{\text{float}} &= \frac{k_B T_e}{e}\ln\left(\frac{A_w + A_e}{A_w}\sqrt{\frac{2\pi m_e}{M}}\right) \end{aligned} \tag{75}$$

The influence of the ion mass $M = N\,\text{u}$ ($\text{u} = 1.66 \cdot 10^{-27}\,\text{kg}$ is the atomic mass unit) on Φ_{float} is shown in Fig. 9. O_2 has a mass of 32 u while a large molecule like HMDSO has a mass of 162 u. It can be seen that the potential does not increase a lot with higher ion masses and for large molecules one has to have in mind that they are cracked into smaller ones in the plasma so that the real floating potential will not be far above the one of oxygen.

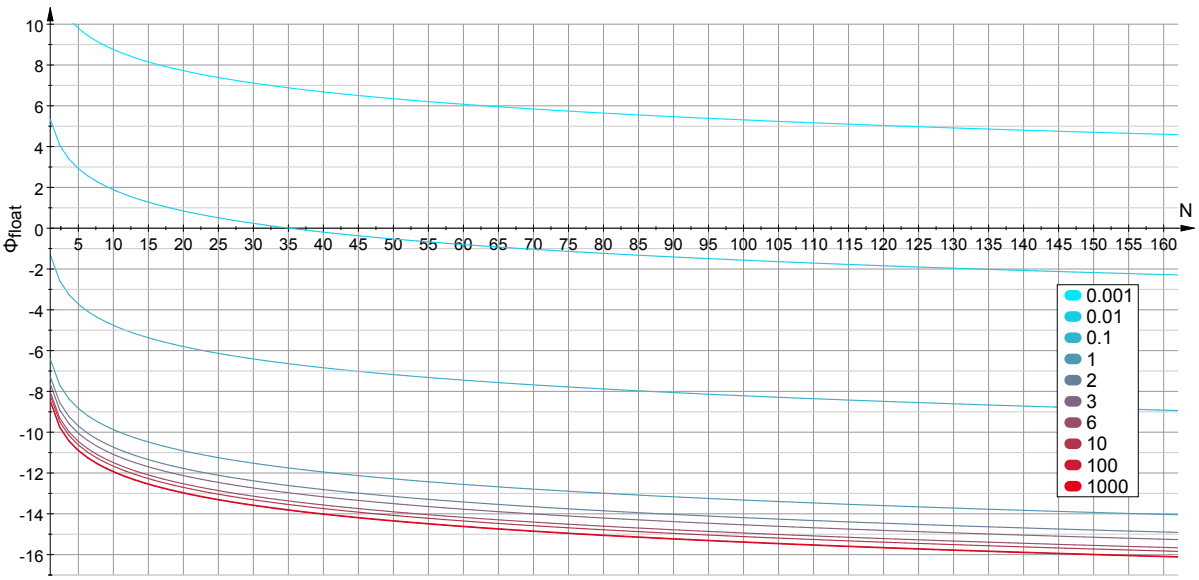

Figure 9: Φ_{float} in V in dependence of the ion mass $M = N\,\text{u}$ for different fractions $\frac{A_w}{A_e}$. The electron temperature was set in the calculation to $T_e = 3.48 \cdot 10^4\,\text{K}$.

As the ions must have the Bohm velocity, the potential to accelerate the ions to the velocity is the plasma potential:

$$\begin{aligned} e\,\Phi_{\text{plasma}} &= \frac{M v_B^2}{2} \\ \Phi_{\text{plasma}} &= \frac{k_B T_e}{2e} \end{aligned} \tag{76}$$

For a typical electron temperature of $T_e = 3.48 \cdot 10^4\,\text{K}$ we have $\Phi_{\text{plasma}} \approx 1.5\,\text{V}$.

Conclusion

The floating potential is often greater than the voltage across the sheath of a grounded chamber wall. Assuming we have a setup with $A_w = 6A_e$ and measure $U_{\text{bias}} = 400\,\text{V}$ we can calculate with (47) that $U_w \approx 4.5\,\text{V}$. If the electrode area is much larger than the chamber wall area the plasma potential can be positive.

By measuring the floating potential with e. g. a LANGMUIR probe, we could measure the electron temperature and could then calculate plasma potential, the real sheath thickness s according to (29) and also the real plasma density n_0 according to (34).

5. Dissipated Power

The power in a CCP is dissipated because energy is consumed to ionize molecules, the ions collide and therefore loose energy and the electrons are accelerated. So in summary we can write

$$P = \int E\,\mathrm{d}t = \int \left(E_{\text{ionization}} + E_{e,\,\text{therm}} + E_{\text{sheath}}\right)\,\mathrm{d}t \tag{77}$$

The power can in principle be split into an ohmic and a stochastic part.

5.1. Ohmic

The ohmic part describes the heating of the plasma due to the RF-electrical field accelerating charged particles. The equation of motion is

$$m\ddot{x} + m\nu\dot{x} = eE_0 \sin(\omega_{\text{RF}} t) \tag{78}$$

where m is the mass of a particle, ν the collision rate of the particles and E_0 the applied field strength.

The power is the energy per time t and the energy is the force along a path x:

$$P_{\text{ohm,\,particle}}(t) = \frac{F(t)\,\mathrm{d}x}{\mathrm{d}t} = eE_0 \sin(\omega_{\text{RF}} t)\dot{x} \tag{79}$$

$\dot{x}$ can be derived by solving (78). It is

$$\dot{x} = -\frac{eE_0\omega_{\text{RF}}}{m\left(\omega_{\text{RF}}^2 + \nu^2\right)} \left(\cos(\omega_{\text{RF}} t) - \frac{\nu}{\omega_{\text{RF}}} \sin(\omega_{\text{RF}} t)\right) \tag{80}$$

so that we get for a single particle

$$\begin{aligned} \bar{P}_{\text{ohm,\,particle}} &= \frac{\omega_{\text{RF}}}{2\pi} \int_0^{2\pi/\omega_{\text{RF}}} P_{\text{ohm,\,particle}}\,\mathrm{d}t \\ &= \frac{e^2 E_0^2}{2m} \frac{\nu}{\omega_{\text{RF}}^2 + \nu^2} \end{aligned} \tag{81}$$

The power per volume is simply

$$\begin{aligned} \bar{P}_{\text{ohm}} &= \bar{P}_{\text{ohm, particle}} \cdot n_0 \\ &= \frac{n_0 e^2 E_0^2}{2m} \frac{\nu}{\omega_{\text{RF}}^2 + \nu^2} \end{aligned} \tag{82}$$

This result can be interpreted by splitting it into a part of the electric field and one of the energy transfer rate due to the collisions:

$$\begin{aligned} \bar{P}_{\text{ohm}} &= \frac{\epsilon_0 E_0^2}{2} \cdot \underbrace{\frac{n_0 e^2}{m\epsilon_0}}_{\omega_{\text{plasma}}^2} \frac{\nu}{\omega_{\text{RF}}^2 + \nu^2} \\ &= \underbrace{\frac{\epsilon_0 E_0^2}{2}}_{\text{electric field}} \cdot \underbrace{\frac{\omega_{\text{plasma}}^2 \, \nu}{\omega_{\text{RF}}^2 + \nu^2}}_{\text{collisions}} \end{aligned} \tag{83}$$

((5) was used.)

The collision term shows that the ohmic heating is maximal if the collision rate $\nu = \dfrac{v}{\lambda}$ is equal to the applied frequency ω_{RF}.

It is interesting to see how electrons and ions are heated. We take as example an argon plasma ($M = 40\,\text{u}$) and $\omega_{\text{RF}} = 85.2\,\text{MHz}$. With (5) we get

$$\frac{\omega_i}{\omega_e} = \sqrt{\frac{m_e}{M}} = 3.7 \cdot 10^{-3} \tag{84}$$

Within the plasma bulk the ions must have the Bohm velocity so that we get with (15) and (22) for the ion collision rate

$$\nu_i = \frac{v_B}{\lambda_i} = \sqrt{\frac{k_B T_e}{\lambda_i^2 M}} = \sqrt{\frac{T_e 2\pi^2 D^4 p^2}{k_B T^2 M}} \tag{85}$$

Putting (75) into (72) leads to

$$\nu_e = \frac{\langle v_{e,\,\text{therm}} \rangle}{\lambda_e} = \frac{A_w}{A_w + A_e} \sqrt{k_B T_e M} \, \frac{1}{2\pi m_e \lambda_e} \tag{86}$$

With (85) we get

$$\begin{aligned} \frac{\nu_i}{\nu_e} &= \frac{\lambda_e}{\lambda_i} \frac{2\pi m_e}{M} \frac{A_w + A_e}{A_w} \\ &= \frac{R_i^2}{R_e^2} \frac{2\pi m_e}{M} \frac{A_w + A_e}{A_w} \\ &= \frac{8\pi m_e}{M} \frac{A_w + A_e}{A_w} \approx 3.4 \cdot 10^{-4} \frac{A_w + A_e}{A_w} \end{aligned} \tag{87}$$

where R is the radius of the of the cross-sectional area. For ions this is twice the molecule radius so that $R_i = d$ (d is the diameter of the molecule). For electrons the cross sectional area is just the area of the molecules ($R_e = d/2$) because the radius of the electron can be neglected compared to the one of molecules.

Assuming $A_w \gg A_e$ and using the fact that $\omega_{\mathrm{RF}} \gg \nu_i$ ($\nu_{i\,\mathrm{Ar}\,2\,\mathrm{Pa}} \approx 300\,\mathrm{kHz}$) we get

$$\begin{aligned}
\bar{P}_{\mathrm{ohm}} &= \bar{P}_{\mathrm{ohm}\,e} + \bar{P}_{\mathrm{ohm}\,i} \\
&= \frac{\epsilon_0 E_0^2}{2}\left(\frac{\omega_e^2\,\nu_e}{\omega_{\mathrm{RF}}^2+\nu_e^2} + \frac{\omega_i^2\,\nu_i}{\omega_{\mathrm{RF}}^2+\nu_i^2}\right) \\
&= \frac{\epsilon_0 E_0^2}{2}\frac{\omega_e^2\nu_e}{\omega_{\mathrm{RF}}^2+\nu_e^2}\left(1 + \frac{\omega_i^2\,\nu_i\,(\omega_{\mathrm{RF}}^2+\nu_e^2)}{\omega_e^2\nu_e\,(\omega_{\mathrm{RF}}^2+\nu_i^2)}\right) \\
&\approx \frac{\epsilon_0 E_0^2}{2}\frac{\omega_e^2\nu_e}{\omega_{\mathrm{RF}}^2+\nu_e^2}\left(1 + \frac{8\pi m_e^2\,(\omega_{\mathrm{RF}}^2+\nu_e^2)}{M^2}\frac{}{\omega_{\mathrm{RF}}^2}\right) \\
&\approx \frac{\epsilon_0 E_0^2}{2}\frac{\omega_e^2\nu_e}{\omega_{\mathrm{RF}}^2+\nu_e^2}\left(1 + 4.7\cdot 10^{-9}\left(1 + \underbrace{\frac{\nu_e^2}{\omega_{\mathrm{RF}}^2}}_{\ll 4.7\cdot 10^9}\right)\right) \\
&\approx \frac{\epsilon_0 E_0^2}{2}\frac{\omega_e^2\nu_e}{\omega_{\mathrm{RF}}^2+\nu_e^2}
\end{aligned} \tag{88}$$

This shows that almost all energy is used to heat the electrons. This result was expected because we derived in sec. 1 that only the electrons can follow the applied RF-frequency while the ions are too heavy and therefore have an eigenfrequency lower than the RF-frequency.

Another interpretation of (82) is to use the relation

$$P = \frac{\sigma}{2}E_0^2 \tag{89}$$

where σ is the electric conductivity:

$$\bar{P}_{\mathrm{ohm}} = \underbrace{\underbrace{\frac{n_0 e^2}{M\nu}}_{\sigma_{\mathrm{DC}}}\frac{\nu^2}{\omega_{\mathrm{RF}}^2+\nu^2}}_{\sigma_{\mathrm{RF}}}\frac{E_0^2}{2} \tag{90}$$

Conclusions

For a pure argon plasma ($M \approx 40\,\mathrm{u}$) at $p = 2\,\mathrm{Pa}$ we have $\lambda_i \approx 8.97\,\mathrm{mm}$. For a typical electron temperature of $T_e = 3.48{\cdot}10^4\,\mathrm{K}$ we get $\nu_i = 299.8\,\mathrm{kHz}$. Assuming $n_0 = 10^{15}\,1/\mathrm{m}^3$

we get $\omega_{\text{plasma}} \approx \omega_i = 6.6\,\text{MHz}$. Fig. 10 shows the energy transfer rate

$$\text{rate} = \frac{\omega_{\text{plasma}}^2\,\nu}{\omega_{\text{applied}}^2 + \nu^2} \tag{91}$$

which is the collision term from (83). For our example we have rate ≈ 1800, $\sigma_{DC} = 1.29 \cdot 10^{-3}\,1/\Omega\text{m}$ (this is about 1/12 of the conductivity of normal saline (0.9 % NaCl in water)) and $\sigma_{\text{RF}} = 4.9 \cdot 10^{-4}\,\sigma_{DC}$.

Fig. 10 also shows what happens for other applied frequencies. According to (61) the plasma density is proportional to the applied frequency and according to (5) the plasma frequency is proportional to the plasma density

$$\begin{aligned} n_0 \approx n_i &\propto \frac{1}{\omega_{\text{applied}}^2} \\ \omega_{\text{plasma}} &\propto \sqrt{n_0} \propto \frac{1}{\omega_{\text{applied}}} \end{aligned}$$

This leads to

$$\frac{\omega_{\text{plasma}}}{\omega_{\text{applied}}} \propto \frac{1}{\omega_{\text{applied}}^2} \tag{92}$$

According to (85) the collision rate is proportional to the electron temperature which is according to (63) in turn proportional to the applied frequency

$$\begin{aligned} T_e &\propto \frac{1}{\omega_{\text{applied}}^5} \\ \nu_i &\propto \sqrt{T_e} \propto \frac{1}{\omega_{\text{applied}}^{2.5}} \end{aligned}$$

This leads to

$$\frac{\nu_i}{\omega_{\text{applied}}} \propto \frac{1}{\omega_{\text{applied}}^{3.5}} \tag{93}$$

For ω_{applied} in the range of GHz we go to the left and downwards in the plot in Fig. 10. So the energy transfer rate becomes negligible. This is again the result that the ions can not be heated because they cannot follow the applied frequency. This results in a globally cold plasma. For ω_{applied} in the range of kHz, we go to the right and upwards in the plot.

5.2. Stochastic

The stochastic part of the dissipated power is difficult to calculate. This power is consumed by the electrons colliding with the moving sheath walls. Within the plasma bulk the electron distribution is a Maxwell-Boltzmann distribution but at the sheath borders this is not the case because a fraction of the electrons are entering the sheath and

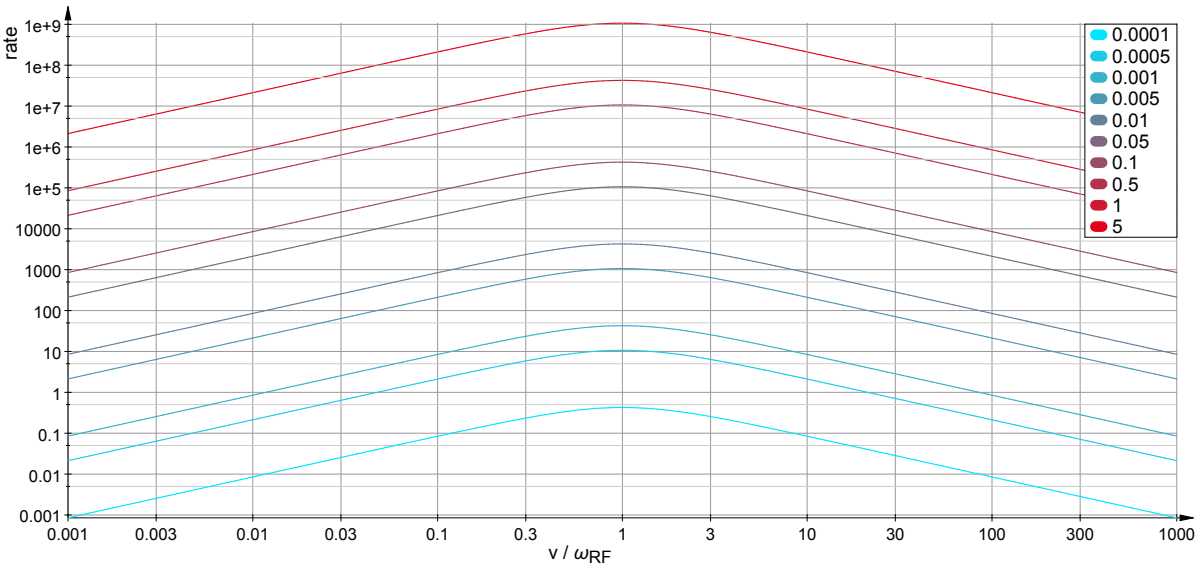

Figure 10: Energy transfer rate in dependency of $\nu/\omega_{\text{applied}}$ (x-axis) and $\omega_{\text{plasma}}/\omega_{\text{applied}}$ (different curves).

will be accelerated. It can even be shown (see [1, sec. "Randschicht mit homogenem Ionendichteprofil"]) that the assumption of a MAXWELL-BOLTZMANN distribution would give that no power is dissipated but measurements show that power is dissipated also at very low pressures (where ohmic dissipation can be neglected). Finding an usable electron distribution is an active research topic and an analytic solution nor a suitable approximation has not yet been found.

6. Electronegative Plasma

Until now we assumed that all ions are positively charged because each ionized atom or molecule looses one or more electrons. This is correct in many cases but the electronegativity of oxygen and fluorine is so high that the O· and F·-radicals can grab two or one electron, respectively. In this case we have also a non-negligible amount of negatively charged ions. The density distributions at a sheath in such an electronegative plasma is shown in Fig. 11. The negative ions are less mobile than the electrons and are therefore pushed more away from the wall. As the result there is no clean sheath border. However, we can define the sheath border at the largest x at which $n_{i-}(x) + n_e(x) = n_0 = n_{i+}(x)$ is fulfilled.

In this case the GAUSS law needs to be modified and is instead of (13)

$$\frac{\mathrm{d}^2\Phi(x)}{\mathrm{d}x^2} = \frac{e}{\epsilon_0}\left(n_e(x) + n_{i-}(x) - n_{i+}(x)\right) \tag{94}$$

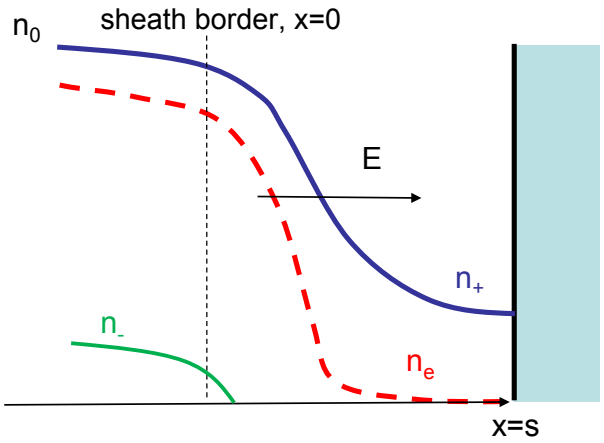

Figure 11: Scheme of the particle densities in a sheath of an electronegative plasma. The wall is at $x = s$, the sheath in the range $0 \leq x \leq s$. Original image from [1].

with $\alpha = \dfrac{n_{i-}}{n_e}$ and $\beta = \dfrac{T_e}{T_i}$ we can solve this and get

$$v_B = \sqrt{\frac{k_B T_e}{M} \frac{1+\alpha}{1+\alpha\beta}} \tag{95}$$

see [1, sec. "Raumladungszone eines elektronegativen Plasmas"] for a detailed derivation.

In our applications we can assume that the electron temperature is much higher than the temperature of the ions ($\beta \gg 1$). In an oxygen plasma we have $\alpha > 0$. The dependence of α on v_B of an oxygen plasma is shown in Fig. 12.

If we use this Bohm velocity in (17) we get instead of (18)

$$\begin{aligned}
\frac{\mathrm{d}E}{\mathrm{d}x} &= = \frac{e\, n_0 \sqrt{\frac{k_B T_e}{M} \frac{1+\alpha}{1+\alpha\beta}}}{\epsilon_0 \sqrt{\frac{e\lambda}{M} E}} \\
\epsilon_0 \sqrt{E}\, \mathrm{d}\, E &= e\, n_0 \sqrt{\frac{k_B T_e}{e\lambda} \frac{1+\alpha}{1+\alpha\beta}}\, \mathrm{d}\, x \\
E(x)^3 &= \frac{9}{4} n_0^2 s^2 \frac{e k_B T_e}{\epsilon_0^2 \lambda} \frac{1+\alpha}{1+\alpha\beta}
\end{aligned} \tag{96}$$

with $E(s) = \dfrac{U}{s}$ we get

$$s = \left(\frac{4U^3 \epsilon_0^2 \lambda}{9 n_0^2 e k_B T_e} \frac{1+\alpha\beta}{1+\alpha} \right)^{1/5} \tag{97}$$

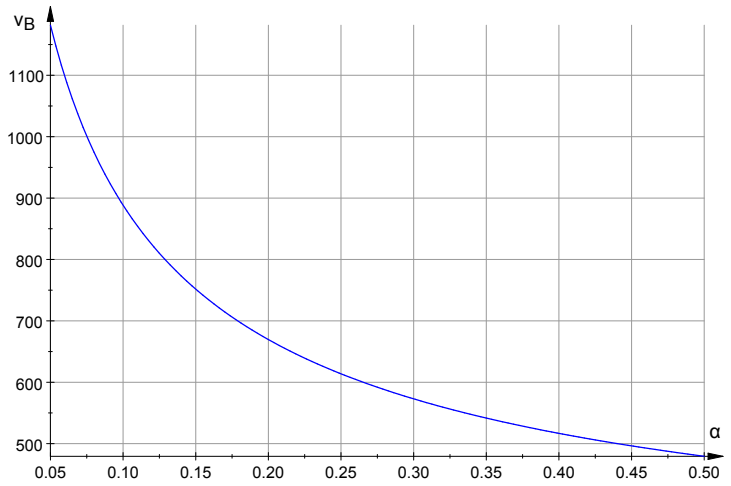

Figure 12: v_B in m/s for an oxygen plasma with a non-negligible fraction of O_2^--ions ($M = 32\,\mathrm{u}$) in dependence of the ion electronegativity $\alpha = \dfrac{n_{i-}}{n_e}$. β was set to $\dfrac{T_e}{T_i} = \dfrac{3.48 \cdot 10^4}{300} = 116$.

Conclusion

With a higher level of electronegativity the Bohm velocity is decreased. This increases the sheath thickness and therefore also the sheath voltage, see the approximation (42).

7. Energy of Impinging Ions

Depending on the substrate it is important to know the energy of the ions impinging the surface. For example for polymer substrates one might estimate what chemical bonds can be cracked by impinging ions.

In the plasma bulk the ions have the Bohm velocity v_B, across the sheath of the electrode there is a mean voltage of U_{bias} along the sheath thickness s. If the substrate is within the plasma bulk the ions are accelerated by the floating potential Φ_{float}. To calculate the ion energies we start with the time-independent equation of motion:

$$M\ddot{x} = eE_0 \tag{98}$$

The sheath can be treated as parallel plate capacitor so that we have $E_0 = \dfrac{U_{\text{bias}}}{s}$

$$M\ddot{x} = \frac{eU_{\text{bias}}}{s} \tag{99}$$

With the knowledge that the ions enter the sheath with the Bohm velocity $v_B = \sqrt{\dfrac{k_B T_e}{M}}$ the integration gives

$$\dot{x}(t) = \frac{eU_{\text{bias}}}{sM}\, t + C \tag{100}$$

$$\dot{x}(t=0) = v_B = C \tag{101}$$

$$\dot{x}(t) = \frac{eU_{\text{bias}}}{sM}\, t + v_B \tag{102}$$

The further integration gives

$$x(t) = \frac{eU_{\text{bias}}}{2sM}\, t^2 + v_B t \tag{103}$$

The acceleration only happens along the sheath thickness s. The time of the acceleration is therefore

$$s = \frac{eU_{\text{bias}}}{2sM}\, \tau^2 + v_B \tau \tag{104}$$

$$0 = \tau^2 + \frac{2sv_B M}{eU_{\text{bias}}}\tau - \frac{2s^2 M}{eU_{\text{bias}}} \tag{105}$$

$$\tau_{1,2} = -\frac{sv_B M}{eU_{\text{bias}}} \pm \sqrt{\left(\frac{sv_B M}{eU_{\text{bias}}}\right)^2 + \frac{2s^2 M}{eU_{\text{bias}}}} \tag{106}$$

The time cannot be negative so that the solution is

$$\begin{aligned}\tau &= -\frac{sv_BM}{eU_{\text{bias}}} + \sqrt{\left(\frac{sv_BM}{eU_{\text{bias}}}\right)^2 + \frac{2s^2M}{eU_{\text{bias}}}} \\ &= -\frac{sv_BM}{eU_{\text{bias}}} + \frac{sM}{eU_{\text{bias}}}\sqrt{v_B^2 + \frac{2eU_{\text{bias}}}{M}} \\ &= \frac{sM}{eU_{\text{bias}}}\left(-v_B + \sqrt{v_B^2 + \frac{2eU_{\text{bias}}}{M}}\right) \end{aligned} \tag{107}$$

Putting this into (102) leads to the final velocity of the ions

$$\begin{aligned} v = \dot{x}(\tau) &= \frac{eU_{\text{bias}}}{sM}\frac{sM}{eU_{\text{bias}}}\left(-v_B + \sqrt{v_B^2 + \frac{2eU_{\text{bias}}}{M}}\right) + v_B \\ &= \sqrt{v_B^2 + \frac{2eU_{\text{bias}}}{M}} = \sqrt{\frac{k_BT_e + 2eU_{\text{bias}}}{M}} \end{aligned} \tag{108}$$

We can now calculate the kinetic energy of the impinging ions:

$$\begin{aligned} E_{\text{kin}} &= \frac{M}{2}v^2 \\ &= \frac{k_BT_e}{2} + eU_{\text{bias}} \end{aligned} \tag{109}$$

Taking into account that the ions can have more than one elementary charge, we get with the number of elementary charges $\tilde{N}$

$$E_{\text{kin}} = \frac{k_BT_e}{2} + \tilde{N}eU_{\text{bias}} \tag{110}$$

We cannot (yet) measure T_e and therefore assume a typical temperature of $T_e = 3.5{\cdot}10^4\,\text{K}$ we get with $\tilde{N} = 1$

$$E_{\text{impinge electrode}} = 1.5 + U_{\text{bias}}\,\text{eV} \tag{111}$$

As the biases are in the range of several 100 V, the influence of the electron temperature can be neglected.

For the case that the substrate is on floating potential we have according to (75)

$$\begin{aligned} E_{\text{impinge floating}} &= -\tilde{N}e\Phi_{\text{float}} \\ &= -\tilde{N}k_BT_e\ln\left(\frac{A_w + A_e}{A_w}\sqrt{\frac{2\pi m_e}{M}}\right) \end{aligned} \tag{112}$$

Example

For an Argon plasma ($M = 40\,\mathrm{u}$ and $\tilde{N} = 1$) in a typical setup ($A_w/A_e = 6$) we have according to (75) $\Phi_{\mathrm{float}} = -13.5\,\mathrm{V}$ and therefore $E_{\mathrm{impinge\,floating}} = 13.5\,\mathrm{eV}$.

Conclusions

We see again that without measuring the electron temperature T_e we cannot calculate the ion energies impinging substrates on floating potential. In contrary for the energy of ions impinging substrates on electrode potential the electron temperature can be neglected.

8. Hollow Cathode Effect

Plasmas with a high density are often observed within recessed volumes like flanges or holes. Their occurrence can be explained geometrically. Taking for example a hole with the radius r, a dense plasma will burn in there if

$$2s > r > s \tag{113}$$

whereas s is the thickness of the sheath. The reason is that the ions impinging the wall generate secondary electrons. They are reflected by the currently negatively charged walls and are accelerated so that they can reach the opposite sheath. There they will again be reflected because of the sheath potential. If both sheath borders are geometrically close together, the electrons can therefore not leave the plasma but will be reflected again and again. This increases the ionization rate enormously because every additional electron can induce an ionization.[7] The effect is illustrated in Fig. 13. It does not usually not occur in holes in substrates at floating potential because the floating potential is much lower than the bias voltage and the holes are in most cases open so that the number of reflections are low until the electrons can leave the hole volume.

We can assume that if $r < s$ no plasma will burn in the holes because then no sheath can be formed. The factor 2 in (113) is an empirical value. If $r \gg s$ the sheath borders are too far away to get the reflecting effect. The electrons are then not directly reflected to the opposite sheath. So the hollow cathode effect only exists for hole radiuses close above the sheath thickness.

Example

A part should be coated at a constant pressure p at a fixed bias of $U_{\mathrm{bias},\,1}$ and later with a lower bias $U_{\mathrm{bias},\,2}$. The values for A_e and A_w are known. In a preliminary test one can measure the dissipated powers P_{measured} at the given bias voltages.

[7] The effect of increasing the ionization rate by holding the electrons in the plasma is also used by the magnetron setup in sputter devices, where the electrons are kept by magnetic field lines.

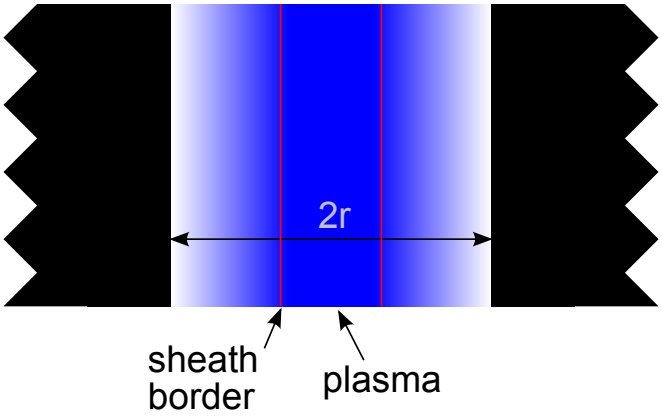

Figure 13: Sketch of a plasma in a hole with the diameter $2r$. The borders of the sheath are so close together that electrons will be reflected directly to the opposite sheath border and therefore remain a long time in the hole resulting in a high ionization rate.

The sheath thickness s can be calculated using the approximation (41). Looking at (45) and (42) we see that

$$\bar{s}^2_{e\,\mathrm{matrix}} = \bar{s}^2_{\mathrm{matrix}} \left(\frac{A_w}{A_e}\right)^2 \tag{114}$$

Using (41) we can write

$$\bar{s}_{e\,\mathrm{matrix}} = \frac{I_{\mathrm{RF}}}{e\, n_0 A_w\, \omega_{\mathrm{RF}}} \frac{A_w}{A_e} \tag{115}$$

putting this into (58) gives

$$\begin{aligned} \bar{s}_{e\,\mathrm{matrix}} &= \frac{1}{e\, n_0 A_w\, \omega_{\mathrm{RF}}} \frac{A_w}{A_e} \left(A_e\, \omega_{\mathrm{RF}}\right)^{2/3} \left(\frac{2\epsilon_0 e n_0 P_{\mathrm{measured}}}{1.146}\right)^{1/3} \\ &= \left(A_e\, \omega_{\mathrm{RF}}\right)^{-1/3} \left(e n_0\right)^{-2/3} \left(\frac{2\epsilon_0 P_{\mathrm{measured}}}{1.146}\right)^{1/3} \end{aligned} \tag{116}$$

putting now (61) into this leads to

$$\begin{aligned} \bar{s}_{e\,\mathrm{matrix}} &= \left(A_e\, \omega_{\mathrm{RF}}\right)^{-1/3} \left(\frac{e}{2e\epsilon_0 U^3_{\mathrm{bias}}} \left(\frac{P_{\mathrm{measured}}}{1.146 \cdot A_e\, \omega_{\mathrm{RF}}}\right)^2 \left(\frac{A_w}{A_e}\right)^6\right)^{-2/3} \left(\frac{2\epsilon_0 P_{\mathrm{measured}}}{1.146}\right)^{1/3} \\ &= \frac{2.292\, \epsilon_0\, \omega_{\mathrm{RF}}\, A^5_e\, U^2_{\mathrm{bias}}}{P_{\mathrm{measured}}\, A^4_w} \end{aligned} \tag{117}$$

We see that due to the matrix model, the mean free path λ of the used precursor(s) and thus the pressure does not have an influence on the approximated sheath thickness.

To calculate the minimal hole radius, we use the lower bias and get $\bar{s}_{e\,\mathrm{matrix\,min}}$. The maximal sheath thickness $\bar{s}_{e\,\mathrm{matrix\,max}}$ is calculated using the larger bias. According to

(113) only in holes with a radius in the range of $2\bar{s}_{e\,\mathrm{matrix\,max}} > r > \bar{s}_{e\,\mathrm{matrix\,min}}$ the hollow cathode effect will occur.

Note that for conductive substrates the electrode area is the uncovered surface area of the electrode plus the visible surface area of the substrate. For non conductive substrates the electrode area is only the uncovered surface area of the electrode.

In practice there are often have setups like the one that is schematically shown in Fig. 14. One uses then a substrate holder that reduces the gap to the substrates so that no dense plasma will burn in. With (29) we are able to calculate the required gap.

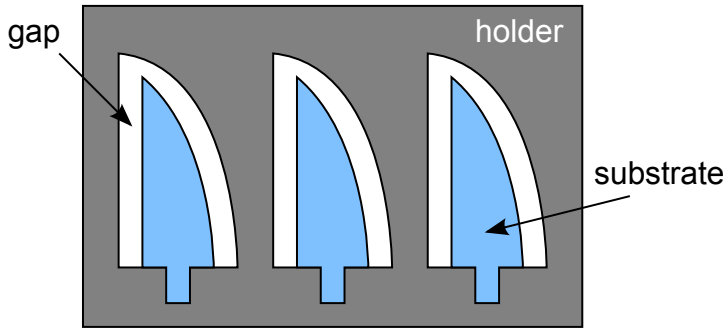

Figure 14: Scheme of a typical sample holder used to coat e. g. knife blades.

9. Conclusions

We see that with the knowledge of the plasma input power P_{measured}, the bias voltage U_{bias} and the electron temperature T_e we are able to explain what is happening in a CCP. But as long as we do not measure T_e we cannot calculate exact values although this is often necessary, e.g. to avoid the hollow cathode effect. We need T_e to be able to calculate

- the sheath thickness s, see (37) – necessary to calculate the diameter of holes in which the hollow cathode effect will occur
- the voltage across a sheath, see (34) – necessary to calculate plasma density and thus the ionization ratio, see (62)
- the floating potential Φ_{floating}, see (75) – necessary to calculate the energy of ions impinging substrates in the plasma bulk

A. Mean Free Paths

The mean free paths λ given here were calculated using the ideal gas law and thus this formula:

$$\lambda = \frac{k_{\text{B}} T}{\sqrt{2}\pi d^2 p} \tag{118}$$

where $k_{\text{B}} = 1.38 \cdot 10^{-23}\,\text{J/K}$ is the BOLTZMANN constant, T the temperature in Kelvin, p the pressure in Pascal and d the largest diameter of the moelcule in meters.

Note: the λ listed in Table 3 are according to $T = 298\,K$ and $p = 1\,\text{Pa}$. For other pressures, the value can be divided by the actual pressure.

The molecule diameter was determined using the program Avogadro by optimizing its geometry in 5000 steps using the Merck molecular force field method 94 (MMFF94). The largest molecule diameter was measured out using the calculated coordinates of the hydrogen molecules the most far away from each other. For hydrogen-free molecules, the atom ccordinates were used plus 2 times the atomic radius of the outermost atoms. Despite that this method is not very precise, it delivers realistic λ for practical use,

Keep in mind, that the λ given in Table 3 are only usable for complete molecules. As soon as a molecule is cracked in the plasma or reacted, its geometry has changed fundamentally and calculations using specific λ are not sensible.

Table 3: Mean free paths λ for some molecules, commonly used in PE-CVD processes; for $T = 298\,K$ and $p = 1\,\mathrm{Pa}$.

Molecule	λ in mm
Gases	
Acetylene	8.4
Ammonia	35.3
Argon	17.9
Carbon tetrafluoride	8.9
Hydrogen	92.6
Methane	29.2
Nitrogen	13.7
Nitrous oxide	
Constitution N≡N−O	6.2
Constitution N=N=O	6.6
Oxygen	16.1
Precursors	
Dimethyldiethoxysilane	2.1
Dimethyldimethoxysilane	1.1
Hexamethyldisilazan	1.6
Hexamethyldisiloxane	1.6
Hexane	1.4
Methyltrimethoxysilane	2.0
Tetraethylorthosilikate	1.1
Tetramethyldisilazane	1.7
Tetramethyldisiloxane	1.7
Tetramethylsilane	3.9
Vinyltrimethoxysilane	2.3

References

[1] A. von Keudell, "Einführung in die Plasmaphysik II: Niedertemperaturplasmen," November 2013. [Online]. Available: https://www.ep2.ruhr-uni-bochum.de/files/skripte/skriptpp2.pdf

[2] ——, "Einführung in die Plasmaphysik," September 2018. [Online]. Available: https://www.ep2.ruhr-uni-bochum.de/files/skripte/skriptpp.pdf